

Chapter 2

Recent Progress in Ribosome Structure Studies

Marat Yusupov

Abstract A high-resolution structure of the eukaryotic ribosome has been determined, leading to increased interest in studying protein biosynthesis and its regulation in the cell. New functional complexes of the full ribosome crystals obtained from the bacteria *Escherichia coli* and *Thermus thermophilus* and the yeast *Saccharomyces cerevisiae* have permitted the identification of precise residue positions in different states of the ribosome function. This knowledge, together with electron microscopy studies, has improved the understanding of how basic ribosome processes, including mRNA decoding, peptide bond formation, mRNA and tRNA translocation, and co-translational transport and modifications of the nascent peptide are regulated.

Keywords Crystal structure • Eukaryotes • Prokaryotes • Protein synthesis • Ribosome

2.1 Introduction

The ribosome is a ribonucleoprotein assembly that is found in all living cells and translates the genetic code into proteins. Recent progress in ribosomal structural biology has included X-ray structure determination and cryo-electron microscopy (EM) studies, which are based on previous knowledge of individual ribosomal components, such as ribosomal RNA, ribosomal proteins, ribosomal subunits, and

M. Yusupov (✉)

Institut de Génétique et de Biologie Moléculaire et Cellulaire, 1 rue Laurent Fries,
BP10142, Illkirch 67400, France

INSERM, U964, Illkirch 67400, France

CNRS, UMR7104, Illkirch 67400, France

Université de Strasbourg, Strasbourg 67000, France

e-mail: marat@igbmc.fr

ribosome complexes in solution (Serdyuk et al. 1983; Wittmann 1983). The shape of the bacterial ribosome and its nonsymmetrical ribosomal subunits was first reconstituted from negatively stained EM images in the laboratories of Vasiliev and Lake (Lake 1976; Vasiliev 1974). Ribosomes from Bacteria and Archaea consist of a large (50S) and a small (30S) subunit, which together constitute the 2.5 megadalton (MDa) 70S ribosome. The eukaryotic counterparts are the 60S and 40S subunits and the 80S ribosome, which range in size from 3.5 MDa in lower eukaryotes to 4.5 MDa in higher eukaryotes. Many key components of the ribosome are conserved across the three kingdoms of life (Bacteria, Archaea, and Eukarya), highlighting their importance in the fundamental process of protein biosynthesis (Melnikov et al. 2012). Protein synthesis has been intensely studied during the past five decades, but for most of this time, the three-dimensional structure of the ribosome remained unclear. Cryo-electron microscopy and single-particle analysis produced the first direct visualizations of the bacterial ribosome in different functional states (Agrawal et al. 1998; Frank et al. 1995; Stark et al. 1997a, b). However, it was not until the X-ray crystallographic structures of the entire 70S ribosome (as well as those of the individual 30S and 50S subunits) began to emerge that accurate atomic models became available (Ban et al. 1998, 1999, 2000; Cate et al. 1999; Clemons et al. 1999; Wimberly et al. 2000; Yusupov et al. 2001). Efforts in ribosome crystallography started early with methods detailing the crystallization of 50S ribosomal subunits isolated from *Bacillus sterothermophilus* and *Haloarcula marismortuae* (Harel et al. 1988; Trakhanov et al. 1987; Yonath et al. 1982, 1983) and the 30S subunit and full ribosome isolated from *Thermus thermophilus* (Trakhanov et al. 1987; Yusupov et al. 1987). The first crystal structures of the 30S subunit from *T. thermophilus* and the 50S subunit from *H. marismortuae* were used to interpret X-ray electron density maps and to model the full ribosome from *T. thermophilus* (Ban et al. 2000; Wimberly et al. 2000; Yusupov et al. 2001). These crystals of individual ribosomal subunits have been used for modeling and in studies of the full ribosome function through complexes with functional ligands, ligand analogues, and antibiotics, as summarized in several review articles (Schmeing and Ramakrishnan 2009; Steitz 2008).

Over the past decade, remarkable advances have been made in full ribosome crystallography, to the extent that it is now possible to obtain a medium- or high-resolution structure of not only the ribosome but also its complexes with key components, such as messenger RNA (mRNA), transfer RNAs (tRNA), and various protein translocation factors (Demeshkina et al. 2012; Dunkle et al. 2011; Jenner et al. 2010a, b; Selmer et al. 2006; Yusupov et al. 2001; Yusupova et al. 2001, 2006). These structural studies can help to explain the mechanism of tRNA binding in the presence of elongation factor Tu (Schmeing et al. 2009), the processes of mRNA decoding (Demeshkina et al. 2012; Schmeing et al. 2011), and the mechanism of GTP hydrolysis (Voorhees et al. 2009), as well as translocation (Dunkle et al. 2011; Gao et al. 2009), termination (Jin et al. 2010, 2011; Korostelev et al. 2008, 2010; Laurberg et al. 2008; Petry et al. 2005; Weixlbaumer et al. 2008; Zhou et al. 2012), and ribosomal recycling (Pai et al. 2008; Weixlbaumer et al. 2007).

Crystallography of full ribosome complexes can also be used for co-translational modification studies (Bingel-Erlenmeyer et al. 2008) and translational regulation (Blaha et al. 2009; Gagnon et al. 2012; Polikanov et al. 2012). Until 2010, only studies concerning the X-ray crystal structures of the bacterial ribosome were available because efforts to elucidate the structure of the eukaryotic ribosome remained unsuccessful.

Crystal structures of the eukaryotic ribosome from *Saccharomyces cerevisiae* were first determined at 4.2 Å and later at 3.0 Å resolution and significantly increased the understanding of protein synthesis and its regulation in the cell (Ben-Shem et al. 2010, 2011).

Recently, the 40S and 60S ribosomal subunits from a eukaryotic organism (*Tetrahymena thermophila*) were successfully crystallized with their protein factors, and the complex structures were determined at 3.8 Å and 3.6 Å resolution, respectively (Klinge et al. 2011; Rabl et al. 2011).

Crystal structures of ribosome complexes also help in the interpretation of lower-resolution data from cryo-EM image reconstructions and can provide a more thorough understanding of ribosomal complexes and their functions. For example, this approach has been used in investigations of the translocation mechanism (Fischer et al. 2010; Fu et al. 2011; Ratje et al. 2010) and protein transport (Becker et al. 2009; Seidelt et al. 2009).

2.2 Structure of the Ribosome

Both the 70S and the 80S ribosomes are asymmetrical assemblies of more than 50 different proteins and three or four RNA chains. Each ribosomal component is present in the ribosome as a single copy, except for stalk proteins (L7 and L12 in bacteria, P proteins in eukaryotes), which are present as four or six copies. Early genetic data, which have been corroborated by structural studies, revealed that the bacterial and eukaryotic ribosomes share a common structural core, comprising 34 conserved proteins (15 in the small subunit and 19 in the large subunit) and approximately 4,400 RNA bases, which together harbor the major functional centers of the ribosomes, including the decoding site, peptidyl-transferase center, and tRNA-binding sites (Smith et al. 2008; Spahn et al. 2001).

Apart from the core (Fig. 2.1), each of the ribosomes contains its own set of specific moieties, including domain-specific proteins, insertions and extensions of conserved proteins, and expansion segments of rRNAs (Gerbi 1986; Lecompte et al. 2002). The 70S ribosome contains 20 bacteria-specific proteins (6 in the 30S subunit, 14 in the 50S subunit), a few extensions of the conserved proteins (for example, S2, S3, and S4), and a few extensions of ribosomal RNA (for example, helices h6, h17, and h33a in 16S rRNA and helices h1 and h68 in 23S rRNA). The 80S ribosome contains 46 eukaryote-specific proteins (18 in the 40S subunit, 28 in the 60S subunit) and extensions and insertions in most of the core proteins, and the

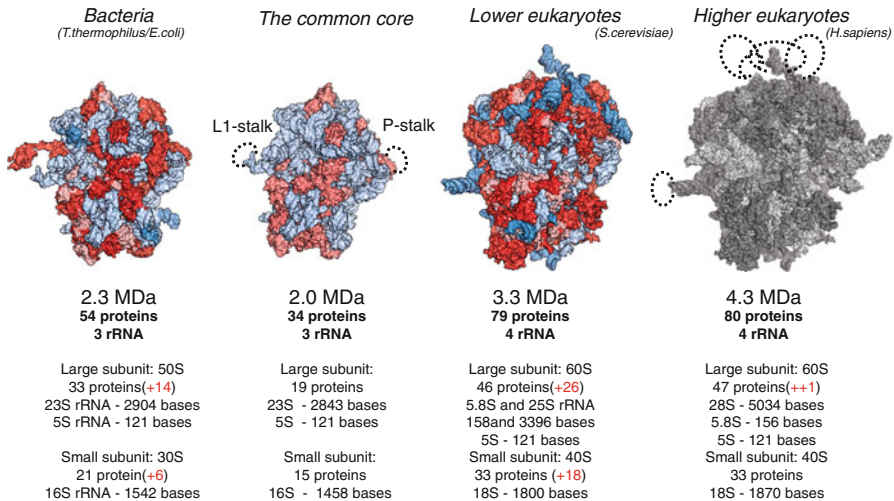


Fig. 2.1 Structures (*top view*) and compositions of bacterial and eukaryotic ribosomes and their common core. Bacterial and eukaryotic ribosomes share a massive conserved core consisting of RNA (*light blue*) and proteins (*light red*). In addition to the core, ribosomes in each domain of life contain their own set of proteins, extensions in conserved proteins (both in *red*), and extensions in ribosomal RNA (in *blue*). 5.8S and 25–28S rRNA are both homologous to 23S rRNA in bacteria. *Dashed lines* around the core indicate the positions of flexible stalks of the ribosomes that are usually disordered in X-ray structures. For simplicity, these lines are not shown on the other structures. The 80S structure of higher eukaryotes has not been determined but is thought to be highly similar to the solved structures of the yeast and *Tetrahymena thermophila* ribosomes. On the panel of human ribosomes, the yeast 80S structure is shown in *grayscale*, and *dashed lines* indicate the positions of long RNA expansion segments, which are the most distinctive feature of ribosomes from higher eukaryotes

rRNA contains several extensions in its conserved chains, with a total length of 900 bases or more. Most of these rRNA and protein moieties envelop the core from the solvent side and are thus accessible for potential interactions with molecular partners, such as translation factors and chaperones. The composition of ribosomes may also vary within bacteria, within eukaryotes, and even within a single species, under different conditions of growth and stress, although to a lesser extent. Within each domain of life, the ribosomes usually contain the same sets of rRNA and protein chains, and divergence is achieved via variations in the length and sequence of ribosomal components, mainly rRNA. In eukaryotes, the size of the 80S ribosome varies within an approximately 1-MDa range, which is largely attributed to insertions in four RNA expansion segments in 25S–28S rRNA (ES7L, ES15L, ES27L, ES39L). In a few cases, ribosomes may contain fewer or additional ribosomal proteins.

The 30S and 40S subunits have similar shapes, including landmarks known as the “head,” “body,” “platform,” and “beak” (Fig. 2.2). The mRNA-binding sites and the three tRNA-binding sites (A, P, and E) are located on the subunit interface. The mRNA enters through a tunnel located between the head and the shoulder and

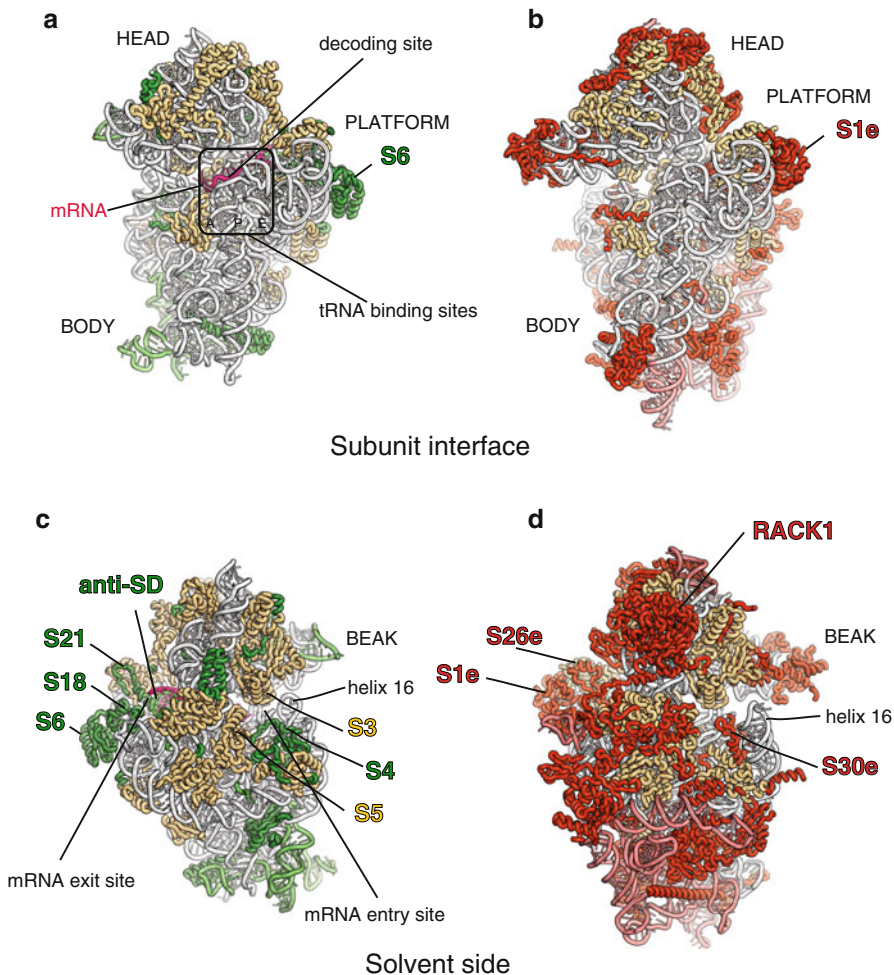


Fig. 2.2 Views of the ribosomal subunits of the yeast ribosome from the perspective of the interface and solvent sides. The head, body, platform, and beak in the small subunit are indicated. The core is colored in *white* (rRNA) and *light orange* (proteins), and domain-specific moieties are in *green* (bacteria) and in *red* (eukaryotes). The tRNA-binding sites are shown as *squares* on the subunit interface

wraps around the neck of the 30S subunit. The mRNA exit site (5'-end of the mRNA) is located between the head and the platform (Jenner et al. 2010a; Yusupova et al. 2001). The decoding center of the small subunit, where the codon and anticodon are paired to ensure fidelity in mRNA decoding, is located on the surface of the interface. In comparing the overall structures, it is evident that there are extensive differences between eukaryotes and bacteria on the solvent side of the small ribosomal subunit (Fig. 2.2). These differences are directly correlated

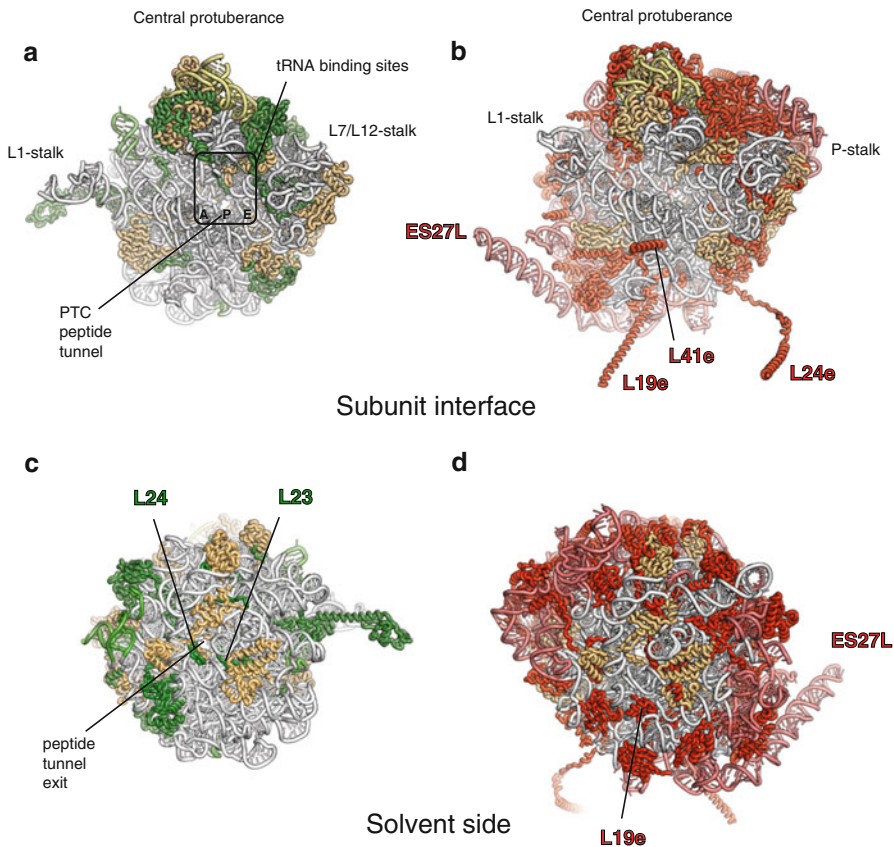


Fig. 2.3 Common and unique features of the 50S and the 60S subunits (*upper* and *lower* pairs, respectively). The central protuberance, L1-stalk, and the L7/L12-stalk (“P-stalk” in eukaryotes) in the large subunit are indicated. Color code as in Fig. 2.2. For simplicity, flexible loop regions are not shown. The tRNA-binding sites are shown as *squares* on the subunit interface

with the considerably more complex pathway of translation initiation that is known to exist in eukaryotic cells.

The 50S and the 60S subunits have similar overall crown-like shapes, which include the “central protuberance,” “L1-stalk,” and the “L7/L12-stalk” (“P-stalk” in eukaryotes) (Fig. 2.3). On the 60S ribosomal subunit, 27 eukaryote-specific proteins, multiple insertions, and extensions of conserved proteins and several rRNA expansion segments are concentrated on the periphery of the subunit, forming a nearly continuous ring-shaped assembly enveloping the core (Fig. 2.3). This ring-shaped assembly comprises two clusters of eukaryote-specific moieties, for which little is known in terms of biological function.

Located on the interface side of the large ribosomal subunit are the three (A, P, and E) tRNA-binding sites and the peptidyl-transferase center, where peptide bond formation is catalyzed. This peptidyl-transferase center is adjacent to the entrance

of a tunnel, along which nascent proteins progress before they emerge from the ribosome on the solvent side. The overall absence of bacteria- and eukaryote-specific moieties on the central regions of both the subunit solvent and interface sides is consistent with the universally conserved functions of these areas. This is seen at the peptidyl-transferase center on the intersubunit surface that is relatively devoid of bacteria- and eukaryote-specific moieties, as well as around the peptide tunnel on the solvent side, which is used for ribosomal association with membranes during protein synthesis (Fig. 2.3). There are, however, important structural differences between the 50S and the 60S subunits, for example, in the organization of the peptide tunnel and the surrounding area, which can be understood in terms of functional divergence.

2.3 Mechanism of Translation

2.3.1 Initiation of Translation

Bacterial and eukaryotic ribosomes use different strategies to recruit mRNA (Fig. 2.4). In bacteria, the 30S subunit directly binds mRNA in the vicinity of the start codon. This process is mediated by the Shine–Dalgarno sequence, a unique feature of bacterial mRNAs that is located upstream of the start codon (Shine and Dalgarno 1974). This sequence interacts with a complementary sequence (anti-Shine–Dalgarno or anti-SD) at the 3'-end of the 16S rRNA, which ensures correct placement of the start codon. Crystal structures of ribosomes in complex with mRNAs reveal that Shine–Dalgarno binding results in formation of a helix, which is located in a cleft on the platform (Jenner et al. 2010a; Yusupova et al. 2001, 2006). In the 30S subunit, the mRNA exit site is surrounded by four of six bacteria-specific proteins: S1, S6, S18, and S21 (Schuwirth et al. 2005; Wimberly et al. 2000). Protein S1 (which is not present in all bacteria) participates in mRNA recruitment to the 30S subunit during translation initiation by binding mRNAs 5'-upstream of their start codon (Hajnsdorf and Boni 2012). The location of S1 on the solvent side of the small subunit was visualized by cryo-EM studies and correlates with its accessibility for mRNAs (Sengupta et al. 2001). The functions of proteins S6, S18, and S21 (which are all located on the platform) (Fig. 2.2) are unclear, although proteins S18 and S21 were suggested to modulate interactions between the Shine–Dalgarno and anti-SD sequences (Yusupova et al. 2001). The location of S21 (which is not present in *T. thermophilus*) in crystal structures of vacant *Escherichia coli* ribosomes slightly overlaps with the Shine–Dalgarno duplex position in ribosome complexes from *T. thermophilus*, suggesting that S21 interacts with the Shine–Dalgarno–anti-SD duplex in *E. coli* (Schuwirth et al. 2005).

In eukaryotes, mRNA is recruited through a unique cap feature at the 5'-end of eukaryotic mRNAs to the 43S pre-initiation complex (which consists of the 40S

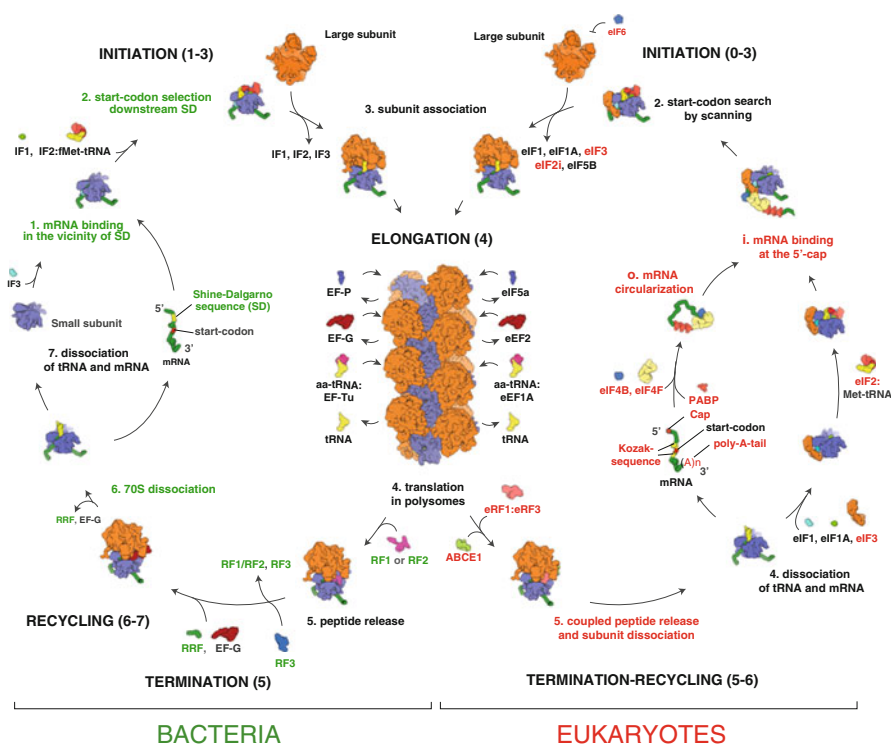


Fig. 2.4 The translation cycle in bacteria and eukaryotes. Translation is a four-stage process that includes initiation, elongation of the polypeptide chain, termination, and recycling of ribosomes. Each of these steps is assisted by protein factors termed initiation (IFs in bacteria or eIFs in eukaryotes), elongation (EF or eEFs), release (RF or eRF), and recycling factors. The elongation step is the most common between bacteria and eukaryotes and is assisted by homologous elongation factors (all homologous factors and common steps of translation are labeled in *black* throughout the figure). During this step, ribosomes assemble in large complexes (termed polysomes), in which the inner shell is typically occupied by the small ribosomal subunit and mRNA and the outer shell is formed by the large ribosomal subunit, from which the nascent peptide emerges during translation. The other steps of translation are unique and include several stages that are different between bacteria (*green*) and eukaryotes (*red*). The initiation, termination, and release factors catalyzing these steps include many nonhomologous proteins that are specific to bacteria (*green*) or eukaryotes (*red*). In eukaryotes, a special group of initiation factors was found to bind mRNA instead of the ribosome

subunit in complex with eIF1, eIF1A, eIF2, eIF3, eIF5, and initiator tRNA) (Fig. 2.4); this results in the formation of a 48S pre-initiation complex. In the 40S subunit, the locations corresponding to the bacterial proteins S6, S18, and S21 are occupied by proteins S1e and S26e. Compared to the 16S rRNA, the 3'-end of the 18S rRNA is shortened and covered by protein S26e (Ben-Shem et al. 2011; Rabl et al. 2011). This finding is consistent with the absence of Shine-Dalgarno sequences in eukaryotic mRNAs.

The solvent side surrounding the mRNA exit site of the 40S subunit contains many unique proteins and rRNA expansion segments that have no analogues in the 30S subunit. Bacteria and eukaryotes employ different strategies to find the mRNA start codon during translation initiation. In bacteria, start-codon selection is dictated by the Shine–Dalgarno sequence and ensures correct positioning of the start codon on the small subunit. In eukaryotes, the start codon may be located several hundred residues downstream from the point of ribosome attachment, and its recognition by the ribosome requires a 5′–3′ mRNA scanning of the ribosome (Aitken and Lorsch 2012; Jackson et al. 2010).

In bacteria, proteins S3, S4, and S5 form the mRNA entry tunnel (Yusupova et al. 2001). At the bacterial ribosome mRNA entry site, the universally conserved helix 16 (h16) of the small ribosomal subunit is held in a conformation in which it is bent toward protein S3 by a bacteria-specific domain of protein S4 that virtually covers a large part of h16 (Fig. 2.2c). However, because this domain does not exist in eukaryotes, h16 is positioned in an entirely different orientation, extending away from the ribosome body (Ben-Shem et al. 2011) (Fig. 2.2d). Although protein S30e is located at the base of h16 in eukaryotes, it does not seem to prevent h16 from adopting different orientations in the 80S structure. This conformational flexibility of h16 is very relevant for the current model of mRNA scanning. This model proposes that the binding of factors eIF1 and eIF1A to the 40S subunit stimulates scanning by inducing h16 to adopt a closed orientation, which stabilizes opening of the mRNA entry tunnel latch (Jackson et al. 2010; Passmore et al. 2007) and allows scanning to take place.

2.3.2 *The Elongation Cycle*

The elongation cycle of protein synthesis in bacteria and eukaryotes is conservative (Fig. 2.4) and contains steps for decoding, peptide bond formation, and translocation. At the beginning of the cycle, the ribosome contains a peptidyl-tRNA with a nascent polypeptide chain in the P-site and an empty A-site. During decoding, the next amino acid is delivered in a ternary complex of elongation factor Tu (EF-Tu), GTP, and aminoacyl-tRNA. Decoding is followed by peptide bond formation, resulting in the elongation of the polypeptide chain by one amino acid. EF-G-catalyzed translocation moves the tRNAs and mRNA with respect to the ribosome. Decoding ensures that the correct aminoacyl-tRNA, as dictated by the mRNA codon, is selected in the A site.

2.3.3 *Mechanism of Decoding: Preliminary Binding*

Base pairing between the mRNA codon and the tRNA anticodon forms the basis for the selection of the correct aminoacyl-tRNA in the A site. The many steps of

decoding have been dissected by pre-steady-state kinetic measurements (Rodnina and Wintermeyer 2001) and single-molecule FRET studies (Blanchard et al. 2004). Kinetic data show that a rapid and reversible initial binding of the ternary complex occurs, followed by a slower codon recognition step. Codon recognition by cognate tRNA leads to an acceleration of GTPase activation and GTP hydrolysis. Thus, tRNA binding induces conformational changes in the ribosomal complex that may be required for GTP hydrolysis by EF-Tu. GTP hydrolysis is followed by the release of EF-Tu and movement (accommodation) of the tRNA into the peptidyl-transferase center, after which peptide bond formation rapidly occurs. Interactions made by three universally conserved bases of the ribosome with the minor groove of the first two base pairs of the codon–anticodon helix stabilize the correct tRNA in the ribosomal A site (Carter et al. 2000; Fourmy et al. 1996; Moazed and Noller 1986). Such a specific interaction of the ribosome with the corresponding base pairs does not occur at the third (wobble) position, which is consistent with the degeneracy of the genetic code.

Early chemical footprinting studies suggested the existence of an A/T state (nonaccommodated state of aminoacyl tRNA of hybrid state model) so long as EF-Tu was present on the ribosome, in which the aminoacyl end of the incoming tRNA cannot enter the peptidyl-transferase center until GTP hydrolysis occurs and EF-Tu has been released, thus ensuring that decoding takes place before peptide bond formation (Moazed and Noller 1989). Single-particle cryo-EM studies of an EF-Tu ribosome complex stalled with kirromycin have directly revealed the existence of the A/T state (Stark et al. 1997b, 2002; Valle et al. 2002, 2003). The structure provides insights into the means by which successful recognition of the cognate codon is signaled by the decoding center of the 30S subunit to the GTPase center of EF-Tu about 80 Å away. This structure may provide a model of how the ribosome might stimulate the GTPase activity of translational GTPases. Although cryo-EM has provided important structural information about the kirromycin-installed decoding complex (Schuette et al. 2009), the 3.6 Å crystal structure of the 70S ribosome from *T. thermophilus* in complex with tRNA^{Phe} in the exit (E) and peptidyl (P) sites, mRNA, and the TC (ternary complex) of EF-Tu•ThrtR-NAThr•GDP, which is stabilized by the antibiotics kirromycin and paromomycin, provides more detailed information about the mechanism of GTP hydrolysis and structural relationships of GTPase activation and codon recognition (Schmeing et al. 2009).

2.3.4 Mechanism of Decoding: Proofreading

At the second step of decoding (proofreading), the ribosome reexamines the tRNA and rejects it if it does not match the codon in the A-site (Rodnina et al. 2005; Zaher and Green 2009). It was suggested that the universally conserved residues G530, A1492, and A1493 of 16S ribosomal RNA, which are critical for tRNA binding in

the A-site (Moazed and Noller 1990; Powers and Noller 1994; Yoshizawa et al. 1999), actively monitor cognate tRNAs (Ogle et al. 2001) and that recognition of the correct codon–anticodon duplex induces an overall ribosome conformational change (domain closure) (Ogle et al. 2002). Recently, a new mechanism for decoding based on six X-ray structures of the 70S ribosome determined at 3.1–3.4 Å resolution, modeling cognate or near-cognate states of the decoding center at the proofreading step, has been suggested. It was shown that the 30S subunit undergoes an identical domain closure upon binding of either cognate or near-cognate tRNA. This conformational change of the 30S subunit forms a decoding center that constrains the mRNA in such a way that the first two nucleotides of the A codon are limited to form Watson–Crick base pairs. When U–G and G–U mismatches, generally considered to form wobble base pairs, are at the first or second codon–anticodon position, the decoding center forces this pair to adopt the geometry close to that of a canonical C–G pair (Fig. 2.5) (Demeshkina et al. 2012). This by itself, or with distortions in the codon–anticodon mini-helix and the anticodon loop, results in the dissociation of the near-cognate tRNA from the ribosome.

The nucleotides A1493, A1492, and G530 of the 16S rRNA in helix 44 (h44 and h18), which contact the first and the second pairs of the codon–anticodon helix, interact with these unusual U4–G36 and G5–U35 pairs in the same manner as they would with the canonical Watson–Crick base pairs C4–G36 and A5–U35 (Fig. 2.6). These findings contradict earlier studies in which these nucleotides were assigned roles in monitoring and discriminating against canonical Watson–Crick pairs in the decoding process (Ogle et al. 2001, 2002). The structures show that G530, A1492, and A1493 form a static part of the decoding center, thereby defining its spatial and stereochemical properties.

During the binding of cognate or near-cognate tRNA to the 70S ribosome, the small subunit undergoes domain closure around the anticodon loop of the tRNA. The closure results in the formation of a tight decoding center that restricts the first two nucleotides of the A codon to form exclusive Watson–Crick base pairs with the tRNA anticodon (Fig. 2.6).

2.3.5 *The Peptide Bond Formation*

The central chemical event in protein synthesis is the peptidyl-transferase reaction, in which the α -amino group of the aminoacyl-tRNA executes a nucleophilic attack on the ester carbon of the peptidyl-tRNA, forming a new peptide bond (Fig. 2.7). The peptidyl-transferase center (PTC) is located on the large ribosomal subunit and is organized by domain V of the ribosomal RNA. Although there are nearly 15 proteins that interact with domain V in the subunit, not a single protein was found within about 18 Å of the PTC, confirming that the ribosome is indeed a ribozyme (Nissen et al. 2000). Structures of the 70S ribosome with three bound tRNA molecules also show that although the L27 protein interacts with the CCA

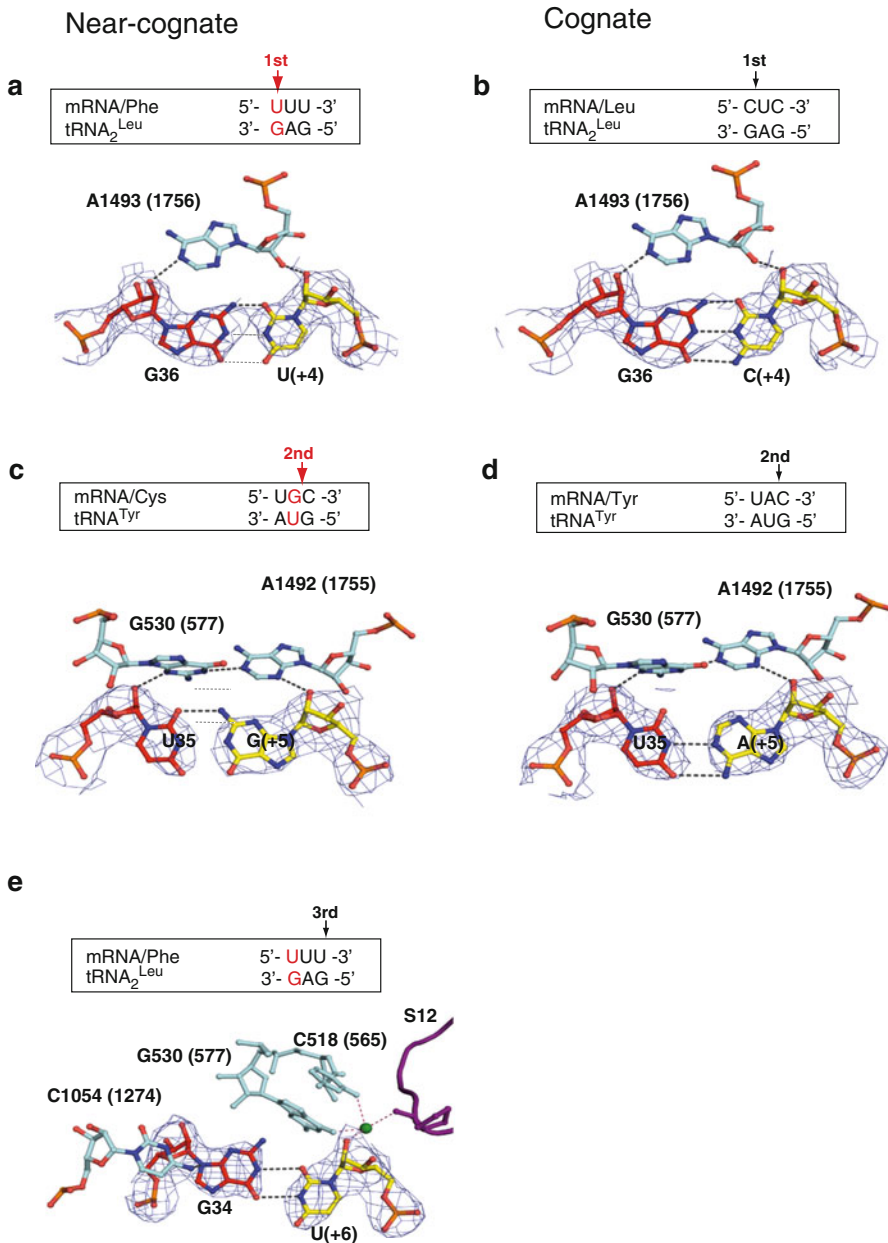


Fig. 2.5 The first and second base pairs of cognate and near-cognate codon–anticodon duplexes have canonical Watson–Crick geometry. The first base pairs of the near-cognate (a) and cognate (b) codon–anticodon duplexes and their interactions with A1493 (A1756) of 16S rRNA. The second base pairs of the near-cognate (c) and cognate (d) codon–anticodon duplexes and their interactions with G530 (G) and A1492 (A1755) of 16S rRNA. The third base pairs of the near-cognate (e) codon–anticodon duplex have a classical wobble geometry. Ribosomal RNA nomenclature of *Escherichia coli* and *Saccharomyces cerevisiae*

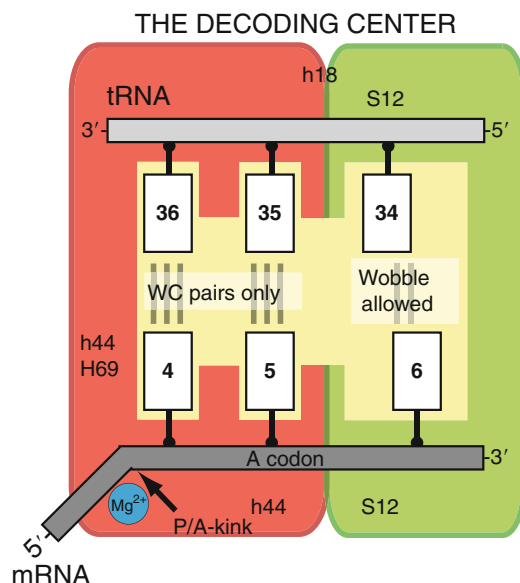


Fig. 2.6 Schematic of the decoding center. The mRNA/tRNA codon–anticodon duplex in the A site is surrounded by helix 44 of 16S RNA and protein S12 of the small ribosomal subunit and helix 69 and helix 18 of the large ribosomal subunit. Together with mRNA, they form a rigged pocket for the incoming anticodon of tRNA. This pocket restricts the first and second position to form exclusively Watson–Crick base pairing but allows the third position to accept wobble base pairing

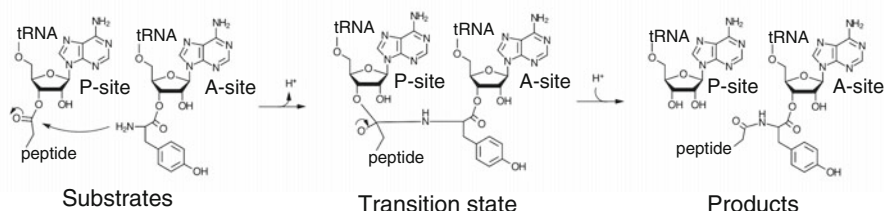


Fig. 2.7 The peptidyl-transferase reaction, including the theoretical transition state. Peptidyl transferase occurs when the α -amino group of the A-site amino acid (in this case, tyrosine) executes a nucleophilic attack on the carboxyl carbon of the P-site nascent peptide C-terminal amino acid. The resulting transition state contains a tetrahedral carbon with a single oxyanion. Subsequent release of the carboxyl carbon from the P-site tRNA yields the reaction products, a deacylated P-site tRNA, and an N + 1 length peptide linked to the A-site tRNA

end of the P-site tRNA, it is not close enough to directly participate in catalyzing the peptide bond formation (Jenner et al. 2010a; Voorhees et al. 2009). The walls of the PTC are composed of the A and P loops, whereas its floor opens up into the exit tunnel, through which the nascent polypeptide chain protrudes (Fig. 2.8a). Several crystal structures of the 50S subunit and 70S ribosome complexed with tRNA or

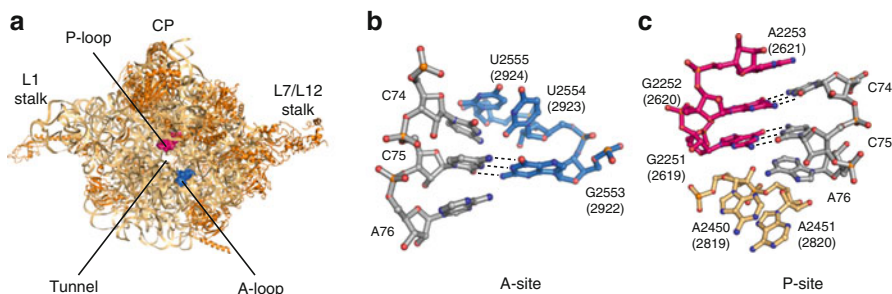


Fig. 2.8 Structure of the ribosomal peptidyl-transferase center (PTC) and the mode of tRNA recognition. **a** Structure of the 50S subunit showing the location of the PTC. The P loop is shown in red; the A loop is shown in blue. The arrow points to the tunnel entrance. rRNA is light brown; the proteins are in gold. **b** The A loop (blue) binds CCA of the A-tRNA (grey). C75 makes Watson–Crick interactions with G2553 (G2922), and C75 base-stacks with U2555 (U2924). **c** The P-loop (red) bases G2252 (G2620) and G2251 (G2619) form Watson–Crick base pairs with C74 and C75 of the peptidyl-tRNA CCA-end (grey), respectively. In **a** and **b**, hydrogen bonds are shown as dashed lines. Ribosomal RNA nomenclature of *E. coli* and *S. cerevisiae*

substrate mimics reveal the means by which the ribosome recognizes its substrates (Fig. 2.8b) (Hansen et al. 2002; Jenner et al. 2010a; Voorhees et al. 2009).

Nucleotide C74 of A tRNA forms a stacking interaction with U2555 and C75 forms a Watson–Crick base pair with G2553, whereas A76 interacts with U2556 and G2583. Similarly, the P-loop binds the CCA end of the P tRNA formed by the Watson–Crick base-pairing of C74 and C75 with G2251 and G2252, respectively. In contrast, A76 stacks onto the ribose of A2451 and creates a hydrogen bond with the O₂' hydroxyl of A2450 (Fig. 2.8c). The CCA ends of the tRNA bound to the A- and the P-sites are related by a 180° rotation, and it has been proposed that this may contribute to the translocation of the peptidyl-tRNA from the A-site to the P-site once the peptide bond is formed. In addition, this relationship may also be necessary for the appropriate positioning of the peptidyl group and the attacking α -amino group. Other interactions have been observed in the PTC of the 70S ribosome from *T. thermophilus*. For instance, the N-terminal tail of the protein L27 interacts with the CCA ends of both tRNAs, thereby stabilizing the conformation (Jenner et al. 2010a, b; Selmer et al. 2006; Voorhees et al. 2009). Although the deletion of the three N-terminal residues from L27 affects the rate of translation (Maguire et al. 2005), this protein is not chemically involved in catalysis. The protein L16 may play a similar role in the eukaryotic ribosome.

2.3.6 Translocation

Translocation is the coupled movement of mRNA and tRNA and follows the formation of each new peptide bond. This step depends on the elongation factor EF-G and is coupled to the hydrolysis of GTP. It is also coupled to large-scale

molecular movements, including the relative rotation of the two ribosomal subunits, thereby emphasizing the structural dynamics of the ribosome. Early studies by Pestka (Pestka 1968) and Spirin (Gavrilova et al. 1976) showed that the poly(U)-dependent synthesis of polyphenylalanine could proceed in the absence of EF-G. These studies suggest that translocation may have originated as a purely ribosomal, factor-independent process. Translocation also appears to depend on the rotation of the 30S subunit relative to the 50S subunit for each step (Frank and Agrawal 2000; Frank et al. 2007; Horan and Noller 2007). Recent single-molecule FRET studies show that spontaneous intersubunit rotation can occur within mRNA-tRNA-ribosome complexes in the absence of EF-G or GTP (Cornish et al. 2008). This finding shows that thermal energy alone is sufficient to drive the intersubunit rotation underlying translocation. Cryo-EM studies and X-ray studies have identified several intermediate states of movement of ribosomal subunits and tRNA during translocation (Fischer et al. 2010; Ratje et al. 2010; Ben-Shem et al. 2011; Dunkle et al. 2011).

2.3.7 Termination and Recycling

Termination occurs when the ribosome reaches the end of the coding region and a stop codon enters the ribosomal A-site. The standard genetic code has three termination codons (UAA, UAG, and UGA). Release factors (class 1) RF1 and RF2 in bacteria and eRF1 in eukaryotes are responsible for recognizing the stop codons in the A-site of the small ribosomal subunit and inducing hydrolysis of the peptidyl-tRNA in the PTC of the large subunit. The factor RF1 recognizes UAG/UAA whereas RF2 recognizes UGA/UAA codons. Factor eRF1 responds to all three codons. All the RFs contain a conserved GGQ motif that is required to trigger peptidyl-tRNA hydrolysis. The mechanism of its action has been studied through X-ray analysis of *T. thermophilus* 70S ribosome complexes (Jin et al. 2010; Korostelev et al. 2008, 2010; Laurberg et al. 2008; Weixlbaumer et al. 2008). Although the crystal structure of eukaryotic eRF1 has been determined, its complex on the ribosome has not yet been elucidated (Song et al. 2000). Release factors (class 2) RF3 in bacteria and eRF3 in eukaryotes are both ribosome-dependent GTPases. The bacterial RF3 does not participate in peptide release but accelerates the dissociation of RF1/RF2 from post-termination ribosomes. The eukaryotic eRF3 strongly stimulates peptide release by eRF1. Recently, the X-ray structure of a ribosome complex containing release factor RF3 was determined for the *T. thermophilus* and *E. coli* ribosome complexes, and a mechanism for the dissociation of class 1 factors by structural rearrangement of the ribosome was suggested (Jin et al. 2011; Zhou et al. 2012).

2.3.8 Polypeptide Exit Tunnel

During translation, the growing peptide chain passes through the peptide exit tunnel to emerge at the solvent side, where it further undergoes processing and folding. In

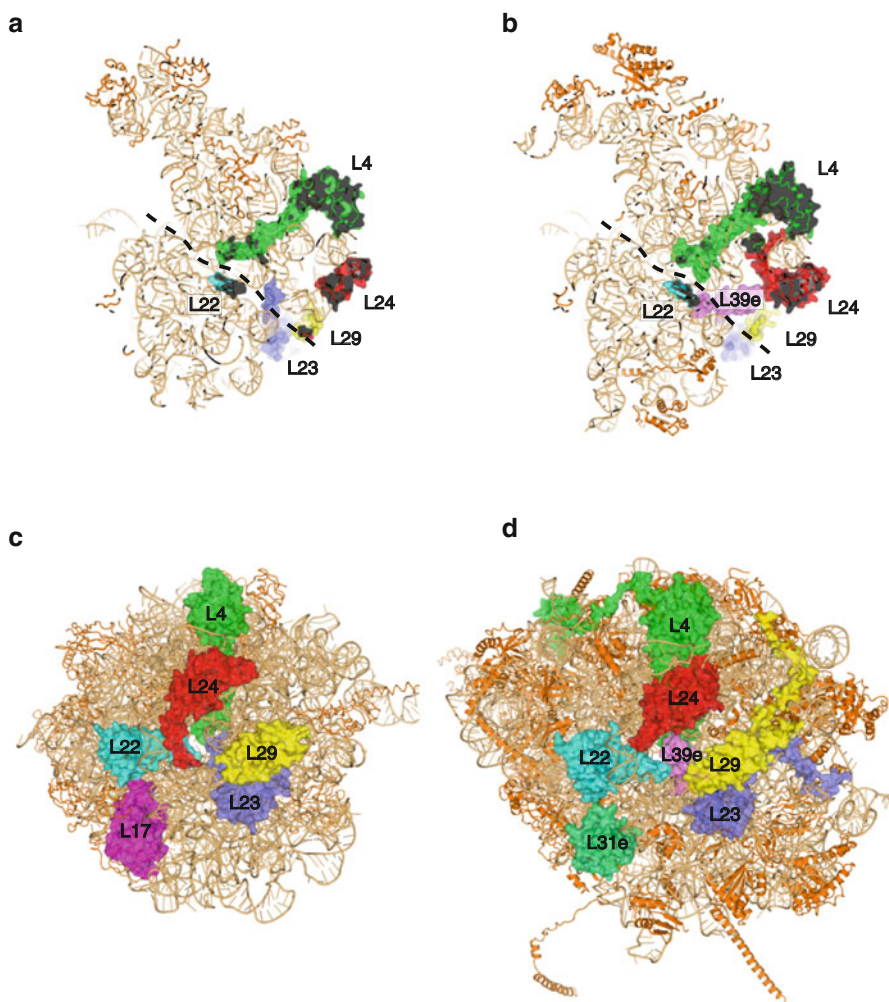


Fig. 2.9 Ribosomal proteins located close to the protein tunnel and exit of the large ribosomal subunits of bacteria and yeast. Protein tunnel in the 50S (a) and 60S (b) subunits. Exit of protein tunnel on the solvent site of the 50S (c) and 60S (d) subunits

bacteria, the tunnel walls are primarily formed by the conserved portions of the 23S rRNA and contain loops of proteins L4, L22, and a bacteria-specific extension of L23 (Fig. 2.9a) (Ban et al. 2000; Harms et al. 2001). In eukaryotes, the area corresponding to the bacteria-specific moieties of L23 overlaps with protein L39e (Fig. 2.9b) (Ben-Shem et al. 2011; Klinge et al. 2011). In both the 50S and the 60S subunits, proteins L4 and L22 form a constriction of the tunnel, located approximately 30 Å from the peptidyl-transferase center. In eukaryotes, the constriction is narrower because of insertions in protein L4. Although the significance of the differences between bacteria and eukaryotes is unclear, it is suggested that the

narrower size of the constriction in eukaryotes may block the access of some macrolide antibiotics to the peptidyl-transferase center (Tu et al. 2005; Zaman et al. 2007). These antibiotics are thought to be delivered to the binding site through the tunnel. Genetic studies have shown that an insertion of six amino acids in the loop of L4 in *E. coli* endows its ribosomes with a resistance to larger-size macrolides, which is similar to the phenomenon observed in eukaryotes.

On the solvent side, the rim of the polypeptide exit tunnel contains several bacteria- or eukaryote-specific proteins and protein extensions: L17, L32, and an insertion in L24 in bacteria and proteins L19e and L31e in eukaryotes (Fig. 2.9c, d). These differences are partly associated with the differential processing of nascent-chain N-termini in bacteria and eukaryotes. In bacteria, nascent peptides contain a formyl group at the N-terminus as a result of the special modification of aminoacylated initiator tRNA (Met-tRNA^fMet), which is formylated to promote its recognition by initiation factor IF2 (Fig. 2.9). During protein synthesis, the formyl group is cleaved by the bacteria-specific enzyme peptide deformylase, which associates with ribosomes through protein L32 (Bingel-Erlenmeyer et al. 2008). As the initiator Met-tRNA^fMet is not formylated in eukaryotes, the positions corresponding to L17 and L32 on the 60S subunit are occupied by the nonhomologous protein L31e, which is associated with a different activity. In yeast, L31e interacts with the protein zuotin, a component of a eukaryote-specific chaperone complex that is involved in co-translational folding of the growing polypeptide (Peisker et al. 2008).

References

- Agrawal RK, Penczek P, Grassucci RA, Frank J (1998) Visualization of elongation factor G on the *Escherichia coli* 70S ribosome: the mechanism of translocation. *Proc Natl Acad Sci USA* 95:6134–6138
- Aitken CE, Lorsch JR (2012) A mechanistic overview of translation initiation in eukaryotes. *Nat Struct Mol Biol* 19:568–576
- Ban N, Freeborn B, Nissen P, Penczek P, Grassucci RA, Sweet R, Frank J, Moore PB, Steitz TA (1998) A 9 Å resolution X-ray crystallographic map of the large ribosomal subunit. *Cell* 93:1105–1115
- Ban N, Nissen P, Hansen J, Capel M, Moore PB, Steitz TA (1999) Placement of protein and RNA structures into a 5 Å-resolution map of the 50S ribosomal subunit. *Nature (Lond)* 400:841–847
- Ban N, Nissen P, Hansen J, Moore PB, Steitz TA (2000) The complete atomic structure of the large ribosomal subunit at 2.4 Å resolution. *Science* 289:905–920
- Becker T, Bhushan S, Jarasch A, Armache JP, Funes S, Jossinet F, Gumbart J, Mielke T, Berninghausen O, Schulten K et al (2009) Structure of monomeric yeast and mammalian Sec61 complexes interacting with the translating ribosome. *Science* 326:1369–1373
- Ben-Shem A, Jenner L, Yusupova G, Yusupov M (2010) Crystal structure of the eukaryotic ribosome. *Science* 330:1203–1209
- Ben-Shem A, Garreau de Loubresse N, Melnikov S, Jenner L, Yusupova G, Yusupov M (2011) The structure of the eukaryotic ribosome at 3.0 Å resolution. *Science* 334:1524–1529
- Bingel-Erlenmeyer R, Kohler R, Kramer G, Sandikci A, Antolic S, Maier T, Schaffitzel C, Wiedmann B, Bukau B, Ban N (2008) A peptide deformylase-ribosome complex reveals mechanism of nascent chain processing. *Nature (Lond)* 452:108–111

- Blaha G, Stanley RE, Steitz TA (2009) Formation of the first peptide bond: the structure of EF-P bound to the 70S ribosome. *Science* 325:966–970
- Blanchard SC, Gonzalez RL, Kim HD, Chu S, Puglisi JD (2004) tRNA selection and kinetic proofreading in translation. *Nat Struct Mol Biol* 11:1008–1014
- Carter AP, Clemons WM, Brodersen DE, Morgan-Warren RJ, Wimberly BT, Ramakrishnan V (2000) Functional insights from the structure of the 30S ribosomal subunit and its interactions with antibiotics. *Nature (Lond)* 407:340–348
- Cate JH, Yusupov MM, Yusupova GZ, Earnest TN, Noller HF (1999) X-ray crystal structures of 70S ribosome functional complexes. *Science* 285:2095–2104
- Clemons WM Jr, May JL, Wimberly BT, McCutcheon JP, Capel MS, Ramakrishnan V (1999) Structure of a bacterial 30S ribosomal subunit at 5.5 Å resolution. *Nature (Lond)* 400:833–840
- Cornish PV, Ermolenko DN, Noller HF, Ha T (2008) Spontaneous intersubunit rotation in single ribosomes. *Mol Cell* 30:578–588
- Demeshkina N, Jenner L, Westhof E, Yusupov M, Yusupova G (2012) A new understanding of the decoding principle on the ribosome. *Nature (Lond)* 484:256–259
- Dunkle JA, Wang L, Feldman MB, Pulk A, Chen VB, Kapral GJ, Noeske J, Richardson JS, Blanchard SC, Cate JH (2011) Structures of the bacterial ribosome in classical and hybrid states of tRNA binding. *Science* 332:981–984
- Fischer N, Konevega AL, Wintermeyer W, Rodnina MV, Stark H (2010) Ribosome dynamics and tRNA movement by time-resolved electron cryomicroscopy. *Nature (Lond)* 466:329–333
- Fourmy D, Recht MI, Blanchard SC, Puglisi JD (1996) Structure of the A site of *Escherichia coli* 16S ribosomal RNA complexed with an aminoglycoside antibiotic. *Science* 274:1367–1371
- Frank J, Agrawal RK (2000) A ratchet-like inter-subunit reorganization of the ribosome during translocation. *Nature (Lond)* 406:318–322
- Frank J, Verschoor A, Li Y, Zhu J, Lata RK, Radermacher M, Penczek P, Grassucci R, Agrawal RK, Srivastava S (1995) A model of the translational apparatus based on a three-dimensional reconstruction of the *Escherichia coli* ribosome. *Biochem Cell Biol* 73:757–765
- Frank J, Gao H, Sengupta J, Gao N, Taylor DJ (2007) The process of mRNA-tRNA translocation. *Proc Natl Acad Sci USA* 104:19671–19678
- Fu J, Munro JB, Blanchard SC, Frank J (2011) Cryoelectron microscopy structures of the ribosome complex in intermediate states during tRNA translocation. *Proc Natl Acad Sci USA* 108:4817–4821
- Gagnon MG, Seetharaman SV, Bulkeley D, Steitz TA (2012) Structural basis for the rescue of stalled ribosomes: structure of YaeJ bound to the ribosome. *Science* 335:1370–1372
- Gao YG, Selmer M, Dunham CM, Weixlbaumer A, Kelley AC, Ramakrishnan V (2009) The structure of the ribosome with elongation factor G trapped in the posttranslocational state. *Science* 326:694–699
- Gavrilova LP, Kostishkina OE, Kotliansky VE, Rutkevitch NM, Spirin AS (1976) Factor-free (“non-enzymic”) and factor-dependent systems of translation of polyuridylic acid by *Escherichia coli* ribosomes. *J Mol Biol* 101:537–552
- Gerbi SA (1986) The evolution of eukaryotic ribosomal DNA. *Biosystems* 19:247–258
- Hajnsdorf E, Boni IV (2012) Multiple activities of RNA-binding proteins S1 and Hfq. *Biochimie* 94:1544–1553
- Hansen JL, Schmeing TM, Moore PB, Steitz TA (2002) Structural insights into peptide bond formation. *Proc Natl Acad Sci USA* 99:11670–11675
- Harel M, Shoham M, Frolov F, Eisenberg H, Mevarech M, Yonath A, Sussman JL (1988) Crystallization of halophilic malate dehydrogenase from *Halobacterium marismortui*. *J Mol Biol* 200:609–610
- Harms J, Schlutzen F, Zarivach R, Bashan A, Gat S, Agmon I, Bartels H, Franceschi F, Yonath A (2001) High resolution structure of the large ribosomal subunit from a mesophilic eubacterium. *Cell* 107:679–688
- Horan LH, Noller HF (2007) Intersubunit movement is required for ribosomal translocation. *Proc Natl Acad Sci USA* 104:4881–4885

- Jackson RJ, Hellen CU, Pestova TV (2010) The mechanism of eukaryotic translation initiation and principles of its regulation. *Nat Rev Mol Cell Biol* 11:113–127
- Jenner L, Demeshkina N, Yusupova G, Yusupov M (2010a) Structural aspects of messenger RNA reading frame maintenance by the ribosome. *Nat Struct Mol Biol* 17:555–560
- Jenner L, Demeshkina N, Yusupova G, Yusupov M (2010b) Structural rearrangements of the ribosome at the tRNA proofreading step. *Nat Struct Mol Biol* 17:1072–1078
- Jin H, Kelley AC, Loakes D, Ramakrishnan V (2010) Structure of the 70S ribosome bound to release factor 2 and a substrate analog provides insights into catalysis of peptide release. *Proc Natl Acad Sci USA* 107:8593–8598
- Jin H, Kelley AC, Ramakrishnan V (2011) Crystal structure of the hybrid state of ribosome in complex with the guanosine triphosphatase release factor 3. *Proc Natl Acad Sci USA* 108:15798–15803
- Klinge S, Voigts-Hoffmann F, Leibundgut M, Arpagaus S, Ban N (2011) Crystal structure of the eukaryotic 60S ribosomal subunit in complex with initiation factor 6. *Science* 334:941–948
- Korostelev A, Asahara H, Lancaster L, Laurberg M, Hirschi A, Zhu J, Trakhanov S, Scott WG, Noller HF (2008) Crystal structure of a translation termination complex formed with release factor RF2. *Proc Natl Acad Sci USA* 105:19684–19689
- Korostelev A, Zhu J, Asahara H, Noller HF (2010) Recognition of the amber UAG stop codon by release factor RF1. *EMBO J* 29:2577–2585
- Lake JA (1976) Ribosome structure determined by electron microscopy of *Escherichia coli* small subunits, large subunits and monomeric ribosomes. *J Mol Biol* 105:131–139
- Laurberg M, Asahara H, Korostelev A, Zhu J, Trakhanov S, Noller HF (2008) Structural basis for translation termination on the 70S ribosome. *Nature (Lond)* 454:852–857
- Lecompte O, Ripp R, Thierry JC, Moras D, Poch O (2002) Comparative analysis of ribosomal proteins in complete genomes: an example of reductive evolution at the domain scale. *Nucleic Acids Res* 30:5382–5390
- Maguire BA, Beniaminov AD, Ramu H, Mankin AS, Zimmermann RA (2005) A protein component at the heart of an RNA machine: the importance of protein I27 for the function of the bacterial ribosome. *Mol Cell* 20:427–435
- Melnikov S, Ben-Shem A, Garreau de Loubresse N, Jenner L, Yusupova G, Yusupov M (2012) One core, two shells: bacterial and eukaryotic ribosomes. *Nat Struct Mol Biol* 19:560–567
- Moazed D, Noller HF (1986) Transfer RNA shields specific nucleotides in 16S ribosomal RNA from attack by chemical probes. *Cell* 47:985–994
- Moazed D, Noller HF (1989) Intermediate states in the movement of transfer RNA in the ribosome. *Nature (Lond)* 342:142–148
- Moazed D, Noller HF (1990) Binding of tRNA to the ribosomal A and P sites protects two distinct sets of nucleotides in 16 S rRNA. *J Mol Biol* 211:135–145
- Nissen P, Hansen J, Ban N, Moore PB, Steitz TA (2000) The structural basis of ribosome activity in peptide bond synthesis. *Science* 289:920–930
- Ogle JM, Brodersen DE, Clemons WM Jr, Tarry MJ, Carter AP, Ramakrishnan V (2001) Recognition of cognate transfer RNA by the 30S ribosomal subunit. *Science* 292:897–902
- Ogle JM, Murphy FV, Tarry MJ, Ramakrishnan V (2002) Selection of tRNA by the ribosome requires a transition from an open to a closed form. *Cell* 111:721–732
- Pai RD, Zhang W, Schuwirth BS, Hirokawa G, Kaji H, Kaji A, Cate JH (2008) Structural insights into ribosome recycling factor interactions with the 70S ribosome. *J Mol Biol* 376:1334–1347
- Passmore LA, Schmeing TM, Maag D, Applefield DJ, Acker MG, Algire MA, Lorsch JR, Ramakrishnan V (2007) The eukaryotic translation initiation factors eIF1 and eIF1A induce an open conformation of the 40S ribosome. *Mol Cell* 26:41–50
- Peisker K, Braun D, Wolffe T, Hentschel J, Funfschilling U, Fischer G, Sickmann A, Rospert S (2008) Ribosome-associated complex binds to ribosomes in close proximity of Rpl31 at the exit of the polypeptide tunnel in yeast. *Mol Biol Cell* 19:5279–5288
- Pestka S (1968) Studies on the formation of transfer ribonucleic acid-ribosome complexes. 3. The formation of peptide bonds by ribosomes in the absence of supernatant enzymes. *J Biol Chem* 243:2810–2820

- Petry S, Brodersen DE, Murphy FVT, Dunham CM, Selmer M, Tarry MJ, Kelley AC, Ramakrishnan V (2005) Crystal structures of the ribosome in complex with release factors RF1 and RF2 bound to a cognate stop codon. *Cell* 123:1255–1266
- Polikanov YS, Blaha GM, Steitz TA (2012) How hibernation factors RMF, HPF, and YfiA turn off protein synthesis. *Science* 336:915–918
- Powers T, Noller HF (1994) Selective perturbation of G530 of 16 S rRNA by translational miscoding agents and a streptomycin-dependence mutation in protein S12. *J Mol Biol* 235:156–172
- Rabl J, Leibundgut M, Ataide SF, Haag A, Ban N (2011) Crystal structure of the eukaryotic 40S ribosomal subunit in complex with initiation factor 1. *Science* 331:730–736
- Ratje AH, Loerke J, Mikolajka A, Brunner M, Hildebrand PW, Starosta AL, Donhofer A, Connell SR, Fucini P, Mielke T et al (2010) Head swivel on the ribosome facilitates translocation by means of intra-subunit tRNA hybrid sites. *Nature (Lond)* 468:713–716
- Rodnina MV, Wintermeyer W (2001) Fidelity of aminoacyl-tRNA selection on the ribosome: kinetic and structural mechanisms. *Annu Rev Biochem* 70:415–435
- Rodnina MV, Gromadski KB, Kothe U, Wieden HJ (2005) Recognition and selection of tRNA in translation. *FEBS Lett* 579:938–942
- Schmeing TM, Ramakrishnan V (2009) What recent ribosome structures have revealed about the mechanism of translation. *Nature (Lond)* 461:1234–1242
- Schmeing TM, Voorhees RM, Kelley AC, Gao YG, Murphy FVT, Weir JR, Ramakrishnan V (2009) The crystal structure of the ribosome bound to EF-Tu and aminoacyl-tRNA. *Science* 326:688–694
- Schmeing TM, Voorhees RM, Kelley AC, Ramakrishnan V (2011) How mutations in tRNA distant from the anticodon affect the fidelity of decoding. *Nat Struct Mol Biol* 18:432–436
- Schuette JC, Murphy FVT, Kelley AC, Weir JR, Giesebrecht J, Connell SR, Loerke J, Mielke T, Zhang W, Penczek PA et al (2009) GTPase activation of elongation factor EF-Tu by the ribosome during decoding. *EMBO J* 28:755–765
- Schuwirth BS, Borovinskaya MA, Hau CW, Zhang W, Vila-Sanjurjo A, Holton JM, Cate JH (2005) Structures of the bacterial ribosome at 3.5 Å resolution. *Science* 310:827–834
- Seidelt B, Innis CA, Wilson DN, Gartmann M, Armache JP, Villa E, Trabuco LG, Becker T, Mielke T, Schulten K et al (2009) Structural insight into nascent polypeptide chain-mediated translational stalling. *Science* 326:1412–1415
- Selmer M, Dunham CM, Murphy FVT, Weixlbaumer A, Petry S, Kelley AC, Weir JR, Ramakrishnan V (2006) Structure of the 70S ribosome complexed with mRNA and tRNA. *Science* 313:1935–1942
- Sengupta J, Agrawal RK, Frank J (2001) Visualization of protein S1 within the 30S ribosomal subunit and its interaction with messenger RNA. *Proc Natl Acad Sci USA* 98:11991–11996
- Serdyuk IN, Agalarov SC, Sedelnikova SE, Spirin AS, May RP (1983) Shape and compactness of the isolated ribosomal 16 S RNA and its complexes with ribosomal proteins. *J Mol Biol* 169:409–425
- Shine J, Dalgarno L (1974) The 3'-terminal sequence of *Escherichia coli* 16S ribosomal RNA: complementarity to nonsense triplets and ribosome binding sites. *Proc Natl Acad Sci USA* 71:1342–1346
- Smith TF, Lee JC, Gutell RR, Hartman H (2008) The origin and evolution of the ribosome. *Biol Direct* 3:16
- Song H, Mugnier P, Das AK, Webb HM, Evans DR, Tuite MF, Hemmings BA, Barford D (2000) The crystal structure of human eukaryotic release factor eRF1: mechanism of stop codon recognition and peptidyl-tRNA hydrolysis. *Cell* 100:311–321
- Spahn CM, Beckmann R, Eswar N, Penczek PA, Sali A, Blobel G, Frank J (2001) Structure of the 80S ribosome from *Saccharomyces cerevisiae*: tRNA-ribosome and subunit-subunit interactions. *Cell* 107:373–386
- Stark H, Orlova EV, Rinke-Appel J, Junke N, Mueller F, Rodnina M, Wintermeyer W, Brimacombe R, van Heel M (1997a) Arrangement of tRNAs in pre- and posttranslocational ribosomes revealed by electron cryomicroscopy. *Cell* 88:19–28

- Stark H, Rodnina MV, Rinke-Appel J, Brimacombe R, Wintermeyer W, van Heel M (1997b) Visualization of elongation factor Tu on the *Escherichia coli* ribosome. *Nature (Lond)* 389:403–406
- Stark H, Rodnina MV, Wieden HJ, Zemlin F, Wintermeyer W, van Heel M (2002) Ribosome interactions of aminoacyl-tRNA and elongation factor Tu in the codon-recognition complex. *Nat Struct Biol* 9:849–854
- Steitz TA (2008) A structural understanding of the dynamic ribosome machine. *Nat Rev Mol Cell Biol* 9:242–253
- Trakhanov SD, Yusupov M, Agalarov S, Garber M, Ryazantzev S, Tischenko S, Shirokov V (1987) Crystallization of 70S ribosomes and 30S ribosomal subunits from *Thermus thermophilus*. *FEBS Lett* 220:319–322
- Tu D, Blaha G, Moore PB, Steitz TA (2005) Structures of MLSBK antibiotics bound to mutated large ribosomal subunits provide a structural explanation for resistance. *Cell* 121:257–270
- Valle M, Sengupta J, Swami NK, Grassucci RA, Burkhardt N, Nierhaus KH, Agrawal RK, Frank J (2002) Cryo-EM reveals an active role for aminoacyl-tRNA in the accommodation process. *EMBO J* 21:3557–3567
- Valle M, Zavialov A, Li W, Stagg SM, Sengupta J, Nielsen RC, Nissen P, Harvey SC, Ehrenberg M, Frank J (2003) Incorporation of aminoacyl-tRNA into the ribosome as seen by cryo-electron microscopy. *Nat Struct Biol* 10:899–906
- Vasiliev VD (1974) Morphology of the ribosomal 30S subparticle according to electron microscopic data. *Acta Biol Med Ger* 33:779–793
- Voorhees RM, Weixlbaumer A, Loakes D, Kelley AC, Ramakrishnan V (2009) Insights into substrate stabilization from snapshots of the peptidyl transferase center of the intact 70S ribosome. *Nat Struct Mol Biol* 16:528–533
- Weixlbaumer A, Petry S, Dunham CM, Selmer M, Kelley AC, Ramakrishnan V (2007) Crystal structure of the ribosome recycling factor bound to the ribosome. *Nat Struct Mol Biol* 14:733–737
- Weixlbaumer A, Jin H, Neubauer C, Voorhees RM, Petry S, Kelley AC, Ramakrishnan V (2008) Insights into translational termination from the structure of RF2 bound to the ribosome. *Science* 322:953–956
- Wimberly BT, Brodersen DE, Clemons WM Jr, Morgan-Warren RJ, Carter AP, Vonnrhein C, Hartsch T, Ramakrishnan V (2000) Structure of the 30S ribosomal subunit. *Nature (Lond)* 407:327–339
- Wittmann HG (1983) Architecture of prokaryotic ribosomes. *Annu Rev Biochem* 52:35–65
- Yonath A, Mussig J, Wittmann HG (1982) Parameters for crystal growth of ribosomal subunits. *J Cell Biochem* 19:145–155
- Yonath A, Tesche B, Lorenz S, Mussig J, Erdmann VA, Wittmann HG (1983) Several crystal forms of the *Bacillus stearothermophilus* 50 S ribosomal particles. *FEBS Lett* 154:15–20
- Yoshizawa S, Fourmy D, Puglisi JD (1999) Recognition of the codon-anticodon helix by ribosomal RNA. *Science* 285:1722–1725
- Yusupov MM, Trakhanov SD, Barinin VV, Boroviagin BD, Garber MB, Sedelnikova SE, Selivanova OM, Tischenko SV, Shirokov VA, Edintsov MM (1987) Crystallization of the 30S subunits of *Thermus thermophilus* ribosomes. *Dokl Akad Nauk (USSR)* 292:1271–1274
- Yusupov MM, Yusupova GZ, Baucom A, Lieberman K, Earnest TN, Cate JH, Noller HF (2001) Crystal structure of the ribosome at 5.5 Å resolution. *Science* 292:883–896
- Yusupova GZ, Yusupov MM, Cate JH, Noller HF (2001) The path of messenger RNA through the ribosome. *Cell* 106:233–241
- Yusupova G, Jenner L, Rees B, Moras D, Yusupov M (2006) Structural basis for messenger RNA movement on the ribosome. *Nature (Lond)* 444:391–394
- Zaher HS, Green R (2009) Fidelity at the molecular level: lessons from protein synthesis. *Cell* 136:746–762
- Zaman S, Fitzpatrick M, Lindahl L, Zengel J (2007) Novel mutations in ribosomal proteins L4 and L22 that confer erythromycin resistance in *Escherichia coli*. *Mol Microbiol* 66:1039–1050
- Zhou J, Lancaster L, Trakhanov S, Noller HF (2012) Crystal structure of release factor RF3 trapped in the GTP state on a rotated conformation of the ribosome. *RNA* 18:230–240

Regulatory Nascent Polypeptides

Ito, K. (Ed.)

2014, IX, 315 p. 75 illus., 62 illus. in color., Hardcover

ISBN: 978-4-431-55051-8